Dissociation kinetics of Mn2+ complexes of NOTA and DOTA

Bohuslav Drahoš, Vojtěch Kubíček, Celia Bonnet, Petr Hermann, Ivan Lukeš, Éva Tóth

Dissociation kinetics of Mn^{2+} complexes of NOTA and DOTA†

Bohuslav Drahoš,[ab] Vojtěch Kubíček,[a] Célia S. Bonnet,[b] Petr Hermann,[a] Ivan Lukeš*[a] and Éva Tóth*[b]

The kinetics of transmetallation of $[Mn(nota)]^-$ and $[Mn(dota)]^{2-}$ was investigated in the presence of Zn^{2+} (5–50-fold excess) at variable pH (3.5–5.6) by ^1H relaxometry. The dissociation is much faster for $[Mn(nota)]^-$ than for $[Mn(dota)]^{2-}$ under both experimental and physiologically relevant conditions ($t_{\frac{1}{2}}$ = 74 h and 1037 h for $[Mn(nota)]^-$ and $[Mn(dota)]^{2-}$, respectively, at pH 7.4, $c(Zn^{2+}) = 10^{-5}$ M, 25 °C). The dissociation of the complexes proceeds mainly *via* spontaneous ($[Mn(nota)]^-$ $k_0 = (2.6 \pm 0.5) \times 10^{-6}$ s^{-1}; $[Mn(dota)]^{2-}$ $k_0 = (1.8 \pm 0.6) \times 10^{-7}$ s^{-1}) and proton-assisted pathways ($[Mn(nota)]^-$ $k_1 = (7.8 \pm 0.1) \times 10^{-1}$ M^{-1} s^{-1}; $[Mn(dota)]^{2-}$ $k_1 = (4.0 \pm 0.6) \times 10^{-2}$ M^{-1} s^{-1}, $k_2 = (1.6 \pm 0.1) \times 10^3$ M^{-2} s^{-1}). The observed suppression of the reaction rates with increasing Zn^{2+} concentration is explained by the formation of a dinuclear Mn^{2+}–L–Zn^{2+} complex which is about 20-times more stable for $[Mn(dota)]^{2-}$ than for $[Mn(nota)]^-$ (K_{MnLZn} = 68 and 3.6, respectively), and which dissociates very slowly (k_3 ~10^{-5} M^{-1} s^{-1}). These data provide the first experimental proof that not all Mn^{2+} complexes are kinetically labile. The absence of coordinated water makes both $[Mn(nota)]^-$ and $[Mn(dota)]^{2-}$ complexes inefficient for MRI applications. Nevertheless, the higher kinetic inertness of $[Mn(dota)]^{2-}$ indicates a promising direction in designing ligands for Mn^{2+} complexation.

Introduction

Chelates of paramagnetic metal ions (Gd^{3+}, Mn^{2+}, Fe^{3+}) are widely applied and studied as contrast agents (CAs) in magnetic resonance imaging (MRI).[1–5] For the safe use of a metal complex as MRI CA, high thermodynamic stability (high complex stability constant) and kinetic inertness (slow complex dissociation under physiological conditions) are required to prevent the *in vivo* release of free ligand and free metal ion as both are very toxic.[6,7] The kinetic inertness in plasma is related primarily to the displacement of the paramagnetic metal from the complex by endogenous metal ions. The complex dissociation can proceed *via* metal-assisted (direct attack of the competing ion on the complex) or proton-assisted pathways.[7,8] In the case of the widely studied Gd^{3+} complexes, the dissociation kinetics is usually investigated either in strongly acidic media (for DOTA derivatives)[9–12] or in the presence of a high excess of a competing metal ion (mostly for DTPA derivatives).[13–17] These conditions are far from the physiological ones, however, they allow to determine the rates of dissociation which would be too long to investigate under physiological conditions. Further, it allows to compare the kinetic inertness of different complexes studied in a similar way.

Most clinical contrast agents are based on Gd^{3+}. However, there is a great interest in chelates of other paramagnetic metal ions as efficient relaxation agents for MRI applications. Complexes of the divalent manganese ion, possessing five unpaired electrons and slow electron spin relaxation, are appealing alternatives.[18–24] However, the chemistry of Mn^{2+} complexes with polydentate ligands which might be suitable for MRI is little developed in comparison to the chemistry of the Gd^{3+} analogues. In particular, the kinetic aspects of Mn^{2+} complexes are essentially unexplored. The lack of ligand-field stabilization in a high-spin d^5 electron configuration and the lower positive charge make Mn^{2+} complexes thermodynamically less stable than other transition metal ions or Gd^{3+} analogues. In addition, even the Mn^{2+} complexes endowed with a high thermodynamic stability, *e.g.* $[Mn(dtpa)]^{3-}$, were found to be kinetically labile and did not prevent the accumulation of Mn^{2+} in the brain after administration of the agent.[25]

It is evident that the stability criteria for the use of Mn^{2+} complexes can be considered less strict as manganese is an endogenous element. The only Mn^{2+}-based contrast agent in clinical use, $[Mn(dpdp)]^{4-}$, has no inner-sphere water molecule and, thus, it is a weak relaxation agent (only outer-sphere relaxation effect). *In vivo*, it undergoes dissociation and the observed *in vivo* relaxation effect is mainly related to the released free hydrated Mn^{2+}. The role of the ligand is to ensure a slower release of free Mn^{2+} and, thus, to prevent toxicity ($dpdp^{6-}$ = *N*,*N*′-dipyridoxylethylenediamine-*N*,*N*′-diacetate-5,5′-bis-(phosphate)).[20,26]

[a]*Department of Inorganic Chemistry, Faculty of Science, Universita Karlova (Charles University), Hlavova, 2030, 128 43 Prague 2, Czech Republic. E-mail: lukes@natur.cuni.cz; Fax: +420-22195-1253; Tel: +420-22195-1263*

[b]*Centre de Biophysique Moléculaire, CNRS, rue Charles Sadron, 45071, Orléans, France. E-mail: eva.jakabtoth@cnrs-orleans.fr; Fax: +33 238257807; Tel: +33 238257625*

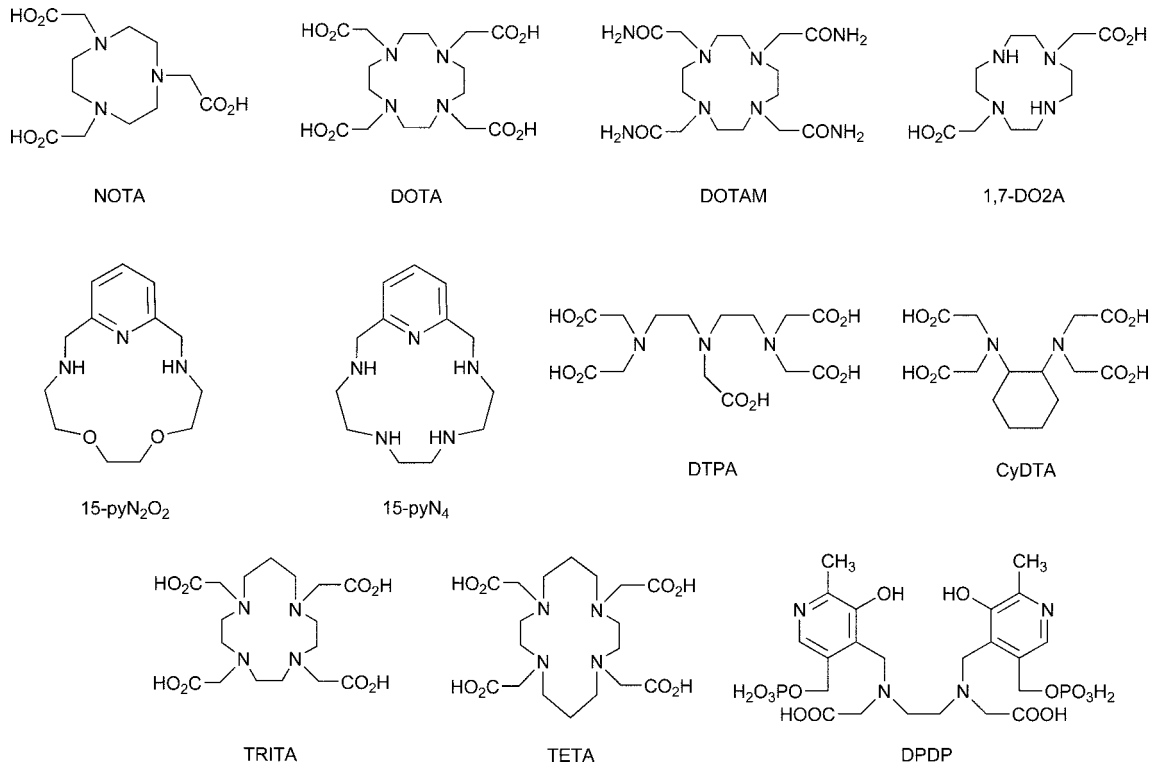

Chart 1 Structure of the ligands studied or discussed in the text.

To the best of our knowledge, there has been only one report on the dissociation of a Mn^{2+} complex.[19] This study, involving the 15-membered pyridine-based macrocycles 15-pyN_4 and 15-pyN_2O_2 (Chart 1), revealed the importance of the proton-assisted dissociation even at physiological pH. More extensive knowledge of the kinetic behavior of Mn^{2+} complexes with various types of ligands could be very helpful in the design of suitable Mn^{2+}-based MRI contrast agents.

In this perspective, here we report a dissociation kinetic study of Mn^{2+} complexes formed with two common polydentate macrocyclic ligands, NOTA and DOTA (Chart 1). None of the complexes is applicable as CA for MRI, as they do not contain any water molecule directly coordinated to the metal ion.[23,27–31] Nevertheless, the results might give insight into the factors determining kinetic inertness of Mn^{2+} complexes in general and, therefore, contribute to the choice of the ligand skeleton most suitable for MRI purposes. These data represent the first dissociation kinetic study of Mn^{2+} chelates formed with this important class of ligands whose complexes with a range of other metal ions are widely employed today in molecular imaging.[2,3]

Experimental

The ligands NOTA and DOTA were purchased from CheMatech and used as received. Deionized water was used for preparation of all solutions. Solutions of the Mn^{2+} complexes were prepared by mixing $MnCl_2$ (410 mM) and NOTA (50.1 mM) or DOTA (46.9 mM) solutions in Mn : L = 1 : 1.05 molar ratio and the pH was adjusted to 8.0 with a diluted NaOH solution. The transmetallation of $[Mn(nota)]^-$ and $[Mn(dota)]^{2-}$ with Zn^{2+} was followed by monitoring the relaxivity at 0.5 MHz on a Stelar SMARTracer fast field-cycling relaxometer (c_{Mn} = 1 mM, 0.02 M *N*-methylpiperazine buffer) in the pH range 3.5–5.6 and in the presence of 5, 10, 20, 30 and 50-fold excess of the exchanging Zn^{2+} at 25 °C and 0.1 M KCl. The relaxivity, r_1, is defined as the paramagnetic enhancement of the longitudinal water proton relaxation rate referred to 1 mM concentration of Mn^{2+}. Each sample was prepared by mixing 1 ml of a buffered $ZnCl_2$ solution of a given concentration with an appropriate amount of $[Mn(nota)]^-$ (c_{Mn} = 41.6 mM) or $[Mn(dota)]^{2-}$ (c_{Mn} = 39.6 mM) stock solution in a 10-mm NMR tube. The experiment time varied according to the pH and corresponded to at least four reaction half-times (*e.g.* for $[Mn(nota)]^-$ at c_{Zn+} = 50 mM and pH 3.5–5.6, the $t_{\frac{1}{2}}$ varied between 1–52 h). Because of the long duration of the experiments, the samples were stored in a thermostat at 25.0 °C between the relaxivity measurements. The pH was measured after each experiment. Parallel control measurements confirmed that the pH was stable during the experiment. The analysis of the experimental data was performed by the Micromath Scientist program (version 2.0, Salt Lake City, UT) using a least-square fitting procedure[32] with a weighting factor of $1/y$.

Protonation constants of NOTA and protonation and stability constants of $[Mn(nota)]^-$ were determined by potentiometric titrations. They were carried out in thermostated vessel at 25 °C and constant ionic strength 0.1 M (NMe_4)Cl using PHM 240 pH-meter, a 2-ml ABU 901 automatic piston burette and a GK 2401B combined electrode (all Radiometer, Denmark). Inert atmosphere was provided by a constant passage of argon saturated with the solvent vapor. The initial volume in the titration cell was 5 ml and the concentration of the ligand was about 0.004 M. Four parallel titrations were carried out for an L : Mn ratio of 1 : 1, with each titration consisting of 40–50 points. The titrations were run in

the –log[H$^+$] range of 1.9–12.0 with an extra HCl added to the starting solution and using (NMe_4)OH solution (~0.2 M) as a base. All equilibria were established quickly. For calculations, the OPIUM software package was used.[33] The value of pK_w was 13.81. The stability constants of the Mn^{2+}–OH^- systems were taken from literature.[34] For more details about potentiometric titrations, see previous papers.[35] In the followings, pH means –log[H$^+$] and all the equilibrium constants are concentration constants.

The ^{1}H NMR titration for the determination of the highest protonation constant (pH range 10.1–13.8, about 15 points) was carried out under conditions close to the potentiometric titrations (no control of ionic strength, 25.0 °C, ligand concentration of about 0.004 M). A coaxial capillary tube with D_2O and *t*-BuOH was used for the lock and referencing. Protonation constants were calculated with OPIUM[33] from the dependence of δ_H of the CH_2 groups on –log[H$^+$].

Results

In order to describe the dissociation kinetics of the $[Mn(nota)]^-$ and $[Mn(dota)]^{2-}$ complexes in a similar way as it is commonly done for Gd^{3+} chelates, we investigated the metal exchange reaction with the diamagnetic Zn^{2+} at variable pH *via* monitoring the release of free Mn^{2+} by relaxometric measurements. At the low magnetic field employed, there is a large difference in the relaxivity of the complex having no inner-sphere water molecule and, thus, possessing only an outer-sphere contribution to the relaxivity,[27] and the free $[Mn(H_2O)_6]^{2+}$ having six water molecules directly coordinated to the metal ion and endowed with a strong inner-sphere relaxivity contribution. In the presence of an excess of the exchanging Zn^{2+} ion, the rate of the reactions can be expressed as shown in eqn (1), where k_{obs} is the pseudo-first-order rate constant, and $[MnL]_{tot}$ is the total concentration of the complex.

$$-\frac{d[MnL]_{tot}}{dt} = k_{obs} \times [MnL]_{tot} \quad (1)$$

The observed dissociation rate constants (k_{obs}) in the pH range 3.5–5.6 and in the presence of 5–50-fold excess of Zn^{2+} are shown in Fig. 1 and 2 and the experimental data are given in ESI (Tables S1–S2).†

For both complexes, the k_{obs} values strongly increase with increasing acid concentration at all concentrations of the exchanging metal ion. On the other hand, the overall dissociation rate decreases with increasing Zn^{2+} concentration. The influence of the increasing concentration of Zn^{2+} ions is less important for pHs close to neutral, while it becomes more visible with decreasing pH. This trend is similar to that reported for several Gd^{3+} chelates.[17] It is related to the formation of dinuclear Mn^{2+}–L–Zn^{2+} species which dissociate more slowly than the protonated MnH_iL species. This effect, reducing the overall dissociation rate, becomes more obvious at lower pH with a higher abundance of the protonated species. For the Mn^{2+}–NOTA system, the thermodynamic stability constant was previously determined from relaxivity measurements[36] or by polarography[37] without indication of protonated species. Here we have investigated this system by potentiometric measurements that revealed the presence of a protonated complex with $\log K_{MnHL}$ = 2.87 (Table 1, for details see ESI Table S3†). Analogously, protonated species have been found in other M^{2+}–NOTA systems (for Mg^{2+} $\log K_{MHL}$ = 4.6, for Ca^{2+} $\log K_{MHL}$ = 5.1 and for Cu^{2+} $\log K_{MHL}$ = 2.7).[38]

For $[Mn(dota)]^{2-}$, two protonated species are known based on potentiometry[30] ($\log K_{MHL}$ = 4.26, $\log K_{MH2L}$ = 2.99; Table 1) and, recently, the X-ray structure of the diprotonated complex with two protonated, uncoordinated acetate arms was also published.[31]

Table 1 Stepwise protonation constants ($\log K_{H_iL}$)[a] of NOTA and DOTA and stability constants ($\log K_{MH_iL}$)[b] of their complexes with Mn^{2+}, Gd^{3+} and Zn^{2+} (25 °C, I = 0.1 M)

Constant[a,b]	NOTA			DOTA		
$\log K_{HL}$	13.17[c]			11.74[d]		
$\log K_{H2L}$	5.74			9.67[d]		
$\log K_{H3L}$	3.22			4.68[d]		
$\log K_{H4L}$	1.96			4.11[d]		
$\log K_{H5L}$	—			2.37[d]		
	Mn^{2+}	Gd^{3+}	Zn^{2+}	Mn^{2+}	Gd^{3+}	Zn^{2+}
$\log K_{ML}$	16.30, 14.9[e], 14.3[f]	13.7[g]	18.3[g]	19.89[h]	24.67[d]	20.8[g]
$\log K_{MHL}$	2.87	3.6[g]	—	4.26[h]	—	4.24[g]
$\log K_{MH2L}$	—	—	—	2.99[h]	—	3.51[g]

[a] Defined as $K_{H_iL} = [H_iL]/[H^+] \times [H_{i-1}L]$ for i = 1–5 [b] $K_{ML} = [ML]/[L]\times[M]$; $K_{MH_iL} = [MH_iL]/[MH_{i-1}L] \times [H^+]$ for i = 1, 2 [c] determined by ^{1}H NMR titration (for details see ESI Table S3, Fig. S3†) [d] ref. 39 [e] ref. 36 [f] ref. 37 [g] ref. 38 [h] ref. 30

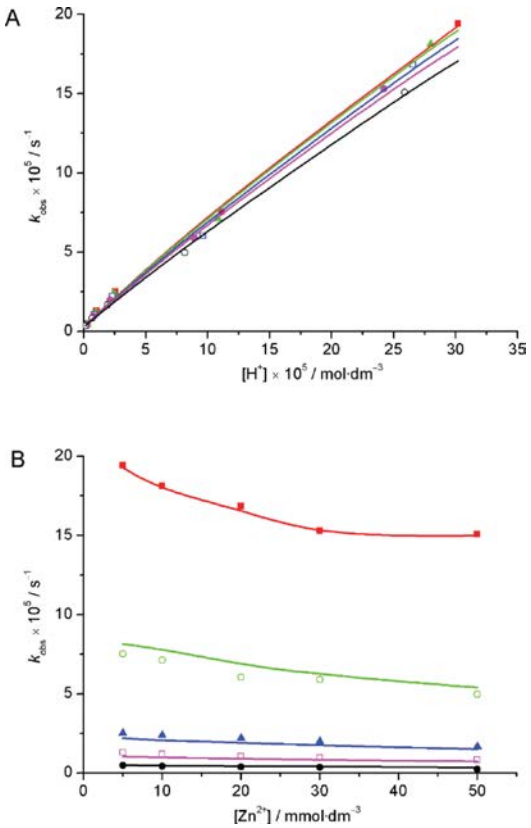

Fig. 1 (a) Dependence of the observed dissociation rate constants for [Mn(nota)]– on proton concentration at Zn^{2+} concentrations of 5 mM (■),10 mM (▲), 20 mM (□), 30 mM (●) and 50 mM (○). (b) Dependence of the observed dissociation rate constants for $[Mn(nota)]^-$ on Zn^{2+} concentration. pH readings from the bottom are 5.6, 5.0, 4.6, 4.0 and 3.5. Parts (a) and (b) are different representations of the same experimental data. The lines correspond to the best fit with the parameters given in Table 2.

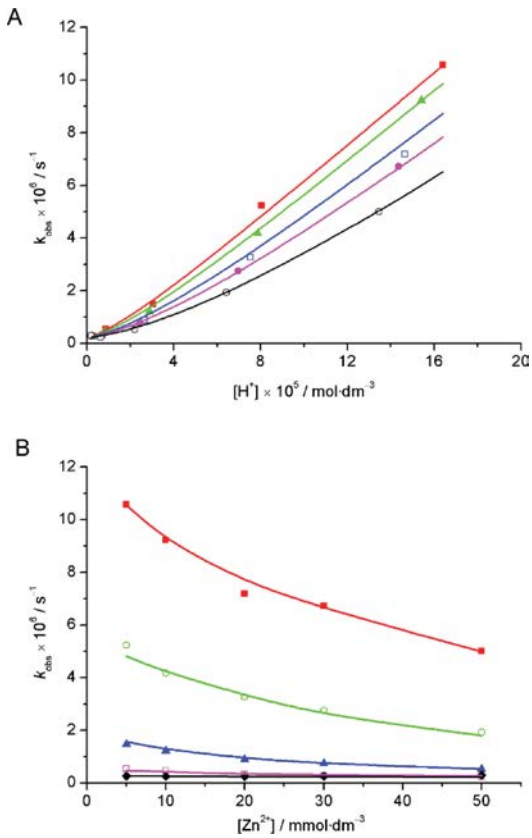

Fig. 2 (a) Dependence of the observed dissociation rate constants for $[Mn(dota)]^{2-}$ on proton concentration at Zn^{2+} concentrations of 5 mM (■), 10 mM (▲), 20 mM (□), 30 mM (●) and 50 mM (○). (b) Dependence of the observed dissociation rate constants for $[Mn(dota)]^{2-}$ on Zn^{2+} concentration. pH readings from the bottom are 5.6, 5.1, 4.6, 4.1 and 3.8. Parts (a) and (b) are different representations of the same experimental data. The lines correspond to the best fit with the parameters given in Table 2.

According to the distribution diagrams (see ESI, Fig. S1 and S2†), in the Mn^{2+}–NOTA system the non-protonated and the monoprotonated complex, whereas in the Mn^{2+}–DOTA system the non-, mono- and diprotonated species are present in solution under the conditions of the kinetic experiments, and these need to be taken into account to describe the overall dissociation rate. In accordance with this, the experimentally observed dependence on the proton concentration of the rate constants is indeed different for $[Mn(nota)]^-$ and $[Mn(dota)]^{2-}$ (Fig. 1a and 2a).

By taking into account the proton- and metal-assisted pathways and the presence of the differently protonated species, the overall dissociation can be illustrated as shown on Scheme 1.

By considering the dissociation pathways in Scheme 1, eqn (2) can be derived for the reaction rate:

$$-\frac{d[\mathrm{MnL}]_{\mathrm{tot}}}{dt} = k_{\mathrm{MnL}}[\mathrm{MnL}] + k_{\mathrm{MnLZn}}[\mathrm{MnLZn}] + k_{\mathrm{MnHL}}[\mathrm{MnHL}] + {}^{\mathrm{H}}k_{\mathrm{MnHL}}[\mathrm{MnHL}][\mathrm{H}^+] + {}^{\mathrm{Zn}}k_{\mathrm{MnHL}}[\mathrm{MnHL}][\mathrm{Zn}^{2+}] + k_{\mathrm{MnH2L}}[\mathrm{MnH_2L}] + {}^{\mathrm{Zn}}k_{\mathrm{MnH2L}}[\mathrm{MnH_2L}][\mathrm{Zn}^{2+}] + {}^{\mathrm{H}}k_{\mathrm{MnH2L}}[\mathrm{MnH_2L}][\mathrm{H}^+] \quad (2)$$

In eqn (2), each term represents a dissociation pathway; ${}^{\mathrm{H}}k_{\mathrm{MnHL}}[\mathrm{MnHL}][\mathrm{H}^+]$ applies only for $[Mn(nota)]^-$ and the last three terms, related to the presence of the diprotonated species, exist only for $[Mn(dota)]^{2-}$. As the overall MnL concentration is the sum of the concentrations of the differently protonated species, eqn (3) and (4) can be derived for the pseudo-first-order rate constants, k_{obs}, of $[Mn(nota)]^-$ and $[Mn(dota)]^{2-}$, respectively; $k_0 = k_{\mathrm{MnL}}$, $k_1 = k_{\mathrm{MnHL}} \cdot K_{\mathrm{MnHL}}$, $k_2 = k_{\mathrm{MnH2L}} \cdot K_{\mathrm{MnHL}} K_{\mathrm{MnH2L}}$ (for $[Mn(dota)]^{2-}$) or $k_2 = K_{\mathrm{MnHL}} \cdot {}^{\mathrm{H}}k_{\mathrm{MnHL}}$ (for $[Mn(nota)]^-$), $k_3 = k_{\mathrm{MnLZn}} \cdot K_{\mathrm{MnLZn}}$, $k_4 = {}^{\mathrm{Zn}}k_{\mathrm{MnHL}} \cdot K_{\mathrm{MnHL}}$, $k_5 = {}^{\mathrm{H}}k_{\mathrm{MnH2L}} \cdot K_{\mathrm{MnHL}} \cdot K_{\mathrm{MnH2L}}$ and $k_6 = {}^{\mathrm{Zn}}k_{\mathrm{MnH2L}} \cdot K_{\mathrm{MnHL}} \cdot K_{\mathrm{MnH2L}}$.

$$k_{\mathrm{obs}} = \frac{\boldsymbol{k_0 + k_1[H^+] + k_2[H^+]^2 + k_3[Zn^{2+}] + k_4[H^+][Zn^{2+}]}}{\boldsymbol{1 + K_{MnHL}[H^+] + K_{MnLZn}[Zn^{2+}]}} \quad (3)$$

$$k_{obs} = \frac{\boldsymbol{k_0 + k_1[H^+] + k_2[H^+]^2 + k_3[Zn^{2+}] + k_4[H^+][Zn^{2+}] + k_5[H^+]^3 + k_6[H^+]^2[Zn^{2+}]}}{\boldsymbol{1 + K_{MnHL}[H^+] + K_{MnH2L}[H^+]^2 + K_{MnLZn}[Zn^{2+}]}} \quad (4)$$

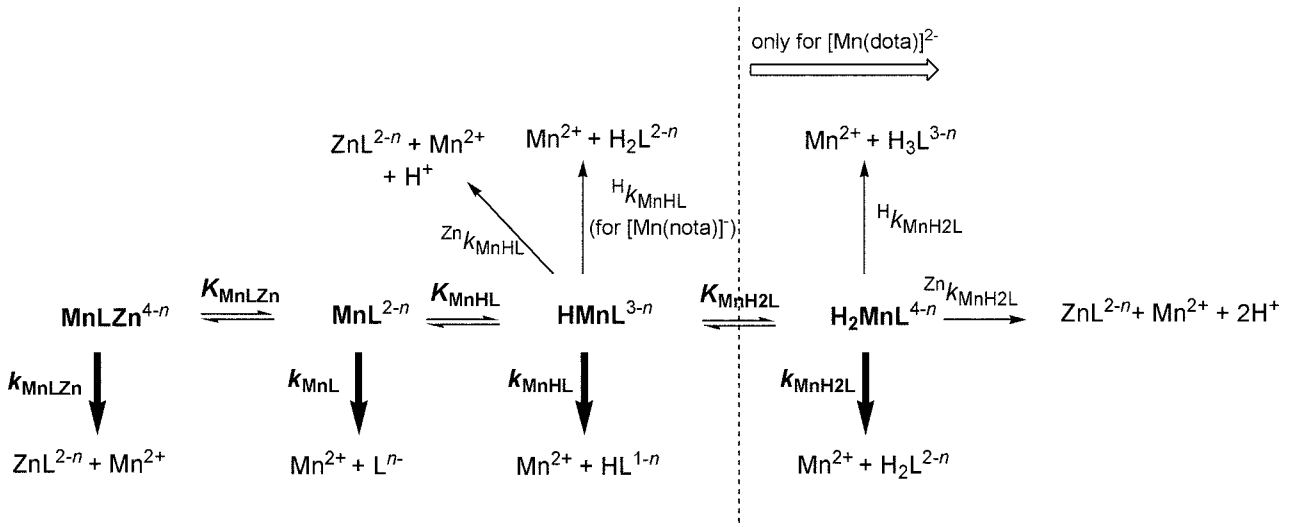

Scheme 1 Possible dissociation pathways for $[Mn(nota)]^-$ and $[Mn(dota)]^{2-}$ (n = 3 for NOTA and n = 4 for DOTA). The pathways having a real contribution to the overall dissociation, as indicated by the fit of the observed rate constants, are represented in bold.

Table 2 Kinetic parameters for the dissociation of $[Mn(nota)]^-$ and $[Mn(dota)]^{2-}$ in comparison to those for $[Mn(15\text{-}pyN_4)]^{2+}$ and analogous Gd^{3+} complexes

Parameters	$[Mn(nota)]^-$	$[Mn(dota)]^{2-}$	$[Mn(15\text{-}pyN_4)]^{2+}$	$[Gd(nota)]^a$	$[Gd(dota)]^{-b}$	$[Gd(dtpa)]^{2-c}$
k_0/s^{-1}	$(2.6 \pm 0.5) \times 10^{-6}$	$(1.8 \pm 0.6) \times 10^{-7}$	—	8.3×10^{-6}	5.0×10^{-10}	—
$k_1/M^{-1}\ s^{-1}$	$(7.8 \pm 0.1) \times 10^{-1}$	$(4.0 \pm 0.6) \times 10^{-2}$	423	2.3×10^{-2}	2.0×10^{-5}	0.58
$k_2/M^{-2}\ s^{-1}$	—[d]	$(1.6 \pm 0.1) \times 10^{3}$	1.0×10^{7}	—	—	9.7×10^{4}
$k_3//M^{-1}\ s^{-1}$	$(1.1 \pm 0.5) \times 10^{-5}$	$(1.5 \pm 0.3) \times 10^{-5}$	—	—	—	5.6×10^{-2}
$k_4/M^{-2}\ s^{-1}$[e]	—[d]	—[d]	1.7×10^{4}	—	—	—
$\log K_{MHL}$	2.87[f]	4.26[f]	4.27	—	—	2
$\log K_{MH2L}$	—[d]	2.99[f]	—	—	—	—
K_{MnLZn}	3.6 ± 0.7	68 ± 6	—	—	—	$K_{GdLZn} = 7$
$t_{\frac{1}{2}}$ (pH 6.0, $c(Zn^{2+}) = 10^{-3}$ M)[g]	58 h	868 h	26 min	23 h	3.7×10^{5} h	3.4 h
$t_{\frac{1}{2}}$ (pH 6.0, $c(Zn^{2+}) = 10^{-5}$ M)[g]	58 h	869 h	27 min	23 h	3.7×10^{5} h	156 h
$t_{\frac{1}{2}}$ (pH 7.4, $c(Zn^{2+}) = 10^{-3}$ M)[g]	74 h	1024 h	11.0 h	23 h	3.8×10^{5} h	3.5 h
$t_{\frac{1}{2}}$ (pH 7.4, $c(Zn^{2+}) = 10^{-5}$ M)[g]	74 h	1037 h	11.4 h	23 h	3.8×10^{5} h	330 h

[a] Ref. 10 [b] 37 °C, transmetallation with Eu^{3+}, ref. 11. [c] Ref. 13. [d] fixed to zero during the fitting procedure [e] k_4 describes the zinc-assisted dissociation of the monoprotonated species [f] fixed to the value obtained from potentiometry [g] calculated on the basis of the reaction rate constants

The observed rate constants for $[Mn(nota)]^-$ and $[Mn(dota)]^{2-}$ were fitted to eqn (3) or (4), respectively, and the calculated parameters are listed in Table 2. In the fit, the protonation constants were fixed to the values determined by potentiometry (Table 1).

We have considered all possible dissociation pathways but the fit of the k_{obs} values showed clearly that several terms have no influence and can be neglected. These include the terms related to the proton- and metal-assisted dissociation of the monoprotonated complex [Mn(Hnota)] (k_2 and k_4), the metal-assisted dissociation of the monoprotonated complex $[Mn(Hdota)]^-$ (k_4), and the proton and metal-assisted dissociation of the diprotonated complex $[Mn(H_2dota)]$ (k_5 and k_6). These terms are indicated in normal type in eqn (3) and (4). Including these dissociation pathways in the fitting led to very small or negative values for the corresponding constants with very large errors.

For $[Mn(nota)]^-$, we could calculate the rate constants k_0 and k_1 corresponding to the spontaneous dissociation of the non-protonated and the protonated complexes as well as a low stability constant for the dinuclear complex, $K_{MnLZn} = 3.6$, which dissociates with a small rate constant k_3 (Table 2, Scheme 1). These results correspond to a close-to-linear dependency of k_{obs} on the proton concentration (Fig. 1a). In the case of $[Mn(dota)]^{2-}$, the fit led to reliable values for k_0, k_1, k_2 (k_2 represents the spontaneous dissociation of the diprotonated complex) as well as to the stability constant of the dinuclear complex, K_{MnLZn}, and the corresponding dissociation rate constant, k_3 (Table 2).

Discussion

The values of k_0 and k_1 are one order of magnitude higher for $[Mn(nota)]^-$ than for $[Mn(dota)]^{2-}$, while the rate constants characterizing the metal-assisted dissociation, k_3, are very similar for both complexes. This difference in k_0 and k_1 accounts for the considerably faster dissociation of $[Mn(nota)]^-$ as expressed by its shorter dissociation half-time calculated for various conditions (Table 2). At physiological pH, the dissociation half-lives do not (or negligibly) depend on the Zn^{2+} concentration, and the contribution of the proton-assisted pathway, represented by k_1, is only 1%. Therefore, under the simulated physiological conditions (pH 7.4 and $c(Zn^{2+}) = 10^{-5}$ M), the overall dissociation proceeds *via* the spontaneous dissociation pathway for both complexes, and the ~15-fold difference in the $t_{1/2}$ values is related to the different k_0 constants.

The mechanism of the spontaneous and the proton-assisted dissociation of $[Mn(nota)]^-$ and $[Mn(dota)]^{2-}$ involves the same intermediates and reaction steps as that of their Gd^{3+} analogues.[10,11] For the spontaneous dissociation of both complexes, the Mn^{2+} ion has to step out from the macrocyclic cavity forming an intermediate ML* species (k_{MnL}, rate-determining step) in which one macrocyclic nitrogen atom is not any more bound to the Mn^{2+} ion. This step is followed by the rapid protonation of a nitrogen of the intermediate (MnHL*) before the fast dissociation to free ligand and metal ion. In the proton-assisted pathway characterized by k_1, $[Mn(nota)]^-$ becomes first protonated on one carboxylate group (HMnL). The carboxylates are known to be labile in this complex[40] and the protonation results in the decoordination of the carboxylic arm. Then, the proton transfer from the carboxylic group to a ring nitrogen atom causes an electrostatic repulsion which removes the Mn^{2+} ion from the macrocyclic cavity (k_{MnHL}, rate-determining step) and initiates the MnHL* dissociation. The proton-assisted dissociation of $[Mn(dota)]^{2-}$ likely proceeds *via* an analogous mechanism, but involves two protonated intermediates, MnHL* and MnH_2L*, with one or two protonated and uncoordinated ring nitrogen atoms, respectively. The rate controlling step is always the formation of the intermediates (MnL*, MnHL* or MnH_2L*).

At higher acidity, the observed dissociation rates for both $[Mn(nota)]^-$ (Fig. 1b) and $[Mn(dota)]^{2-}$ (Fig. 2b) decrease with increasing Zn^{2+} concentration indicating the transitional formation of a slowly dissociating dinuclear Mn^{2+}–L–Zn^{2+}complex. This dinuclear complex competes with the protonated complexes. It dissociates more slowly than the protonated complexes, thus the overall dissociation rate is decreased. This decrease becomes more significant at higher proton concentration where the protonated (or diprotonated) species are more abundant while at low acidity the change in k_{obs} with increasing Zn^{2+} concentration is less important. Consequently, the dissociation half-times calculated for physiological pH do not vary with Zn^{2+} concentration (Table 2). The suppression of the dissociation rate with an excess of the exchanging metal ion has been previously observed for the transmetallation of Gd^{3+} complexes of open-chain (DTPA)[13]

or macrocyclic ligands (TETA, TRITA; Chart 1)[17] with Eu^{3+}. The dissociation kinetic study on the divalent metal complex $[Cd(cydta)]^{2-}$ (Chart 1) with exchanging Pb^{2+} or Cu^{2+} ions also revealed the same trend,[41] and similarly, a dinuclear complex with the exchanging ion bound to the carboxylate pendant arm was proposed to account for this kinetic behaviour.

We can predict a higher tendency for dinuclear complex formation for the more negatively charged $[Mn(dota)]^{2-}$ than for $[Mn(Hdota)]^{-}$ or $[Mn(H_2dota)]^{0}$ with the protonated acetate pendant arm(s). Accordingly, the fitting of the k_{obs} data showed that the zinc-assisted dissociation of both protonated complexes is negligible (*vida supra*). On the other hand, the dependence of k_{obs} on Zn^{2+} concentration is more pronounced for $[Mn(dota)]^{2-}$ than for $[Mn(nota)]^{-}$, corresponding to the higher value of the dinuclear complex stability constant (Table 2). In addition to the higher negative charge, the increased flexibility of the acetate pendant arms in $[Mn(dota)]^{2-}$ also facilitates the approach of Zn^{2+} and contributes to the increased stability of the dinuclear complex. In contrast to the tightly packed structure of $[Mn(nota)]^{-}$, where all three carboxylates are coordinated to the metal ion (CN = 6),[28] the octadentate ligand in $[Mn(dota)]^{2-}$ might have non-coordinated acetate arms available for Zn^{2+} coordination. The crystal structure of $[Mn(dota)]^{2-}$ is not known. For the diprotonated $[Mn(H_2dota)]$ complex, the solid-state structure has been reported; two protonated and non-coordinating acetate arms are present and the metal ion has CN = 6.[31] Six- and seven-coordination are most common for poly(amino carboxylate) Mn^{2+} chelates.[19,42] Only few examples of eight-coordination have been described, including the complex with a DOTA-tetraamide ligand, DOTAM (Chart 1), $[Mn(dotam)]^{2+}$.[31] Even if all four carboxylates are coordinated to the metal ion in $[Mn(dota)]^{2-}$, they will be more flexible and available for the formation of a dinuclear complex than those in $[Mn(nota)]^{-}$.

For the Mn^{2+} complex of the 15-membered pyridine-macrocycle 15-pyN_4,[19] both proton- (k_1, k_2) and zinc-assisted (k_4) dissociation pathways were found to be important, whereas the dissociation of the 15-pyN_2O_2 analogue was instantaneous and could not be studied under the same experimental conditions (pH 4.7–6.0). The rate constants of $[Mn(15\text{-}pyN_4)]^{2+}$ are several orders of magnitude higher than those of $[Mn(nota)]^{-}$ and $[Mn(dota)]^{2-}$, resulting in a much faster overall dissociation (Table 2). Several factors can account for this difference, including the presence of two inner-sphere water molecules in $[Mn(15\text{-}pyN_4)]^{2+}$, its lower thermodynamic stability and the more "open" structure of the aza-crown-ether complexes that might result in different dissociation mechanisms.

For Gd^{3+} chelates, a large body of dissociation kinetic data has been reported which evidence a fundamentally different behavior for the complexes of open-chain, DTPA-derived, and macrocyclic, DOTA-derived ligands. For the dissociation of macrocyclic Gd^{3+} complexes, especially of $[Gd(dota)]^{-}$, strongly acidic conditions had to be usually used because of their considerably high kinetic inertness, mainly related to their tight packing, preorganization and to the high rigidity of the 12-membered macrocycle.[10,11,17] The dissociation was found independent of the exchanging metal ion concentration (when an exchanging metal ion was employed) under these highly acidic conditions, but also at higher pHs (pH = 2–5),[9–11] and only k_0 and k_1 could be determined for [Gd(nota)] and $[Gd(dota)]^{-}$ (for $[Eu(dota)]^{-}$, k_2 was also reported).[11] The k_0 and k_1 values are comparable for [Gd(nota)] and $[Mn(nota)]^{-}$, and $[Mn(nota)]^{-}$ is even more inert under simulated physiological conditions (Table 2). This can likely be accounted for the smaller ionic radius of Mn^{2+} which suits well to the relatively small cavity of the triazacyclononane-based ligand contrary to the larger Gd^{3+} ion with an uncompleted coordination sphere. For the DOTA complexes, the dissociation half-time is several orders of magnitude longer for the Gd^{3+} analogue showing its extraordinary kinetic inertness (Table 2). The Gd^{3+} complexes formed with open-chain ligands are kinetically less inert than those with macrocycles and their dissociation proceeds mainly *via* metal-assisted pathways. The overall dissociation rate of $[Gd(dtpa)]^{2-}$ in the presence of Zn^{2+} [13] is in the same range as those for $[Mn(nota)]^{-}$ or $[Mn(dota)]^{2-}$; however, it shows a much higher dependency on Zn^{2+} concentration even at physiological conditions.

The high kinetic inertness of $[Mn(dota)]^{2-}$ indicates a promising direction in designing ligands for stable Mn^{2+} complexation. The modification of the DOTA scaffold by changing and/or removing some pendant arms can result in a free site for water coordination in a thermodynamically and kinetically stable Mn^{2+} complex. Recently, a relaxivity of $r_1 = 6.2\ mM^{-1}\ s^{-1}$ (20 MHz, 37 °C) has been reported for the Mn^{2+} complex of 1,7-DO2A[31] (Chart 1) which suggests the presence of one inner-sphere water in the complex.

Conclusion

The dissociation kinetic study of $[Mn(dota)]^{2-}$ and $[Mn(nota)]^{-}$ revealed unexpectedly high kinetic inertness, disproving that Mn^{2+} complexes are all kinetically labile. In addition to the high thermodynamic complex stability, the saturation of the coordination sphere of Mn^{2+} exclusively by the ligand donor atoms (no inner-sphere water) can also contribute to this kinetic inertness. The dissociation is strongly pH-dependent and proceeds ~15 times faster for $[Mn(nota)]^{-}$ than for $[Mn(dota)]^{2-}$, under both experimental and physiologically relevant conditions. This difference results from the higher rate constants calculated for the spontaneous and the proton-assisted dissociation, k_0 and k_1, respectively. In the transmetallation with Zn^{2+}, the exchanging metal ion suppresses its own rate of exchange due to the formation of a stable dinuclear Mn^{2+}–L–Zn^{2+} complex which dissociates more slowly than the protonated species. This phenomenon is particularly significant at low pHs where the protonated complexes contribute more actively to the overall dissociation. The effect of the dinuclear complex formation is more significant for $[Mn(dota)]^{2-}$; it is also expressed by a ~20-times higher value of the stability constant of its Mn^{2+}–L–Zn^{2+} complex. Our results suggest that for both complexes the spontaneous dissociation pathway prevails under physiologically relevant H^+ and Zn^{2+} concentration. Given the high kinetic inertness of $[Mn(dota)]^{2-}$, DOTA-type ligands are prime candidates for the development of Mn^{2+}-based MRI probes.

Acknowledgements

We thank Dr J. Havlíčková for the protonation/stability constant measurements. Support from the Grant Agency of the Academy of Science of the Czech Republic (No. KAN201110651) and the Long-Term Research Plan of the Ministry of Education of the Czech Republic (No. MSM0021620857) is acknowledged. B. Drahoš acknowledges the PhD grant of the RFR program

of the French Ministry of Education and Research. The work was carried out in the frame of COST D38 (MŠMT OC 179) and the Grant Agency of the Czech Republic (No. P207/11/1437).

Notes and references

1 E. Terreno, D. D. Castelli, A. Viale and S. Aime, *Chem. Rev.*, 2010, **110**, 3019–3042.
2 *Future Med. Chem.*, 2010, **2**, 305–531. The issue No. 3 is dedicated to "Molecular Probes in Optical and Magnetic Resonance Imaging".
3 S. Aime, D. D. Castelli, S. G. Crich, E. Gianolio and E. Terreno, *Acc. Chem. Res.*, 2010, **42**, 822–831.
4 É. Tóth and A. E. Merbach, *The Chemistry of Contrast Agents in Medical Magnetic Resonance Imaging*, John Wiley & Sons, Chichester, 2001.
5 P. Hermann, J. Kotek, V. Kubíček and I. Lukeš, *Dalton Trans.*, 2008, 3027–3047.
6 J. M. Ideé, M. Port, C. Robic, C. Medina, M. Sabatou and C. Corot, *J. Magn. Reson. Imaging*, 2009, **30**, 1249–1258.
7 E. Brücher and A. D. Sherry, Stability and Toxicity of Contrast Agents, in *The Chemistry of Contrast Agents in Medical Magnetic Resonance Imaging*, É. Tóth and A. E. Merbach ed., Wiley, Chichester, 2001, pp. 243–280.
8 A. D. Sherry, P. Caravan and R. E. Lenkinski, *J. Magn. Reson. Imaging*, 2009, **30**, 1240–1248.
9 X. Wang, T. Jin, V. Comblin, A. Lopez-Mut, E. Merciny and J. F. Desreux, *Inorg. Chem.*, 1992, **31**, 1095–1099.
10 E. Brücher and A. D. Sherry, *Inorg. Chem.*, 1990, **29**, 1555–1559.
11 É. Tóth, E. Brücher, I. Lázár and I. Tóth, *Inorg. Chem.*, 1994, **33**, 4070–4076.
12 P. Caravan, J. J. Ellison, T. J. McMurry and R. B. Lauffer, *Chem. Rev.*, 1999, **99**, 2293–2352.
13 L. Sarka, L. Burai and E. Brücher, *Chem. Eur. J.*, 2000, **6**, 719–724.
14 J. Kotek, F. K. Kálmán, P. Hermann, E. Brucher, K. Binnemans and I. Lukeš, *Eur. J. Inorg. Chem.*, 2006, 1976–1986.
15 Z. Jászberényi, I. Bányai, E. Brücher, R. Király, K. Hideg and T. Kálai, *Dalton Trans.*, 2006, 1082–1091.
16 Z. Baranyai, Z. Pálinkás, F. Uggeri and E. Brücher, *Eur. J. Inorg. Chem.*, 2010, 1948–1956.
17 E. Balogh, R. Tripier, R. Ruloff and É. Tóth, *Dalton Trans.*, 2005, 1058–1065.
18 V. Kubíček and É. Tóth, *Adv. Inorg. Chem.*, 2009, **61**, 63–129.
19 B. Drahoš, J. Kotek, P. Hermann, I. Lukeš and É. Tóth, *Inorg. Chem.*, 2010, **49**, 3224–3238.
20 T. Murakami, R. L. Baron, M. S. Peterson, J. H. III. Oliver, P. L. Davis, B. S. Confer and M. P. Federle, *Radiology*, 1996, **200**, 69–77.
21 S. Aime, P. L. Anelli, M. Botta, M. Brocchetta, S. Canton, F. Fedeli, E. Gianolio and E. Terreno, *JBIC, J. Biol. Inorg. Chem.*, 2002, **7**, 58–67.
22 J. S. Troughton, M. T. Greenfield, J. M. Greenwood, S. Dumas, A. J. Wiethoff, J. Wang, M. Spiller, T. J. McMurry and P. Caravan, *Inorg. Chem.*, 2004, **43**, 6313–6323.
23 E. Balogh, Z. He, W. Hsieh, S. Liu and É. Tóth, *Inorg. Chem.*, 2007, **46**, 238–250.
24 *NMR Biomed.*, 2004, **17**, 527–634. The issue No. 8 is dedicated to the "Manganese Enhanced Magnetic Resonance Imaging (MEMRI)".
25 B. Gallez, C. Baudelet and M. Geurts, *Magn. Reson. Imaging*, 1998, **16**, 1211–1215.
26 S. M. Rocklage, W. P. Cacheris, S. C. Quay, F. E. Hahn and K. N. Raymond, *Inorg. Chem.*, 1989, **28**, 477–485.
27 C. F. G. C. Geraldes, A. D. Sherry, R. D. III. Brown and S. H. Koenig, *Magn. Reson. Med.*, 1986, **3**, 242–250.
28 K. Wieghardt, U. Bossek, P. Chaudhuri, W. Herrmann, B. C. Menke and J. Weiss, *Inorg. Chem.*, 1982, **21**, 4308–4314.
29 Y. Fukuda, M. Hirota, M. Kon-no, A. Nakao and K. Umezawa, *Inorg. Chim. Acta*, 2002, **339**, 322–326.
30 A. Bianchi, L. Calabi, C. Giorgi, P. Losi, P. Mariani, D. Palano, P. Paoli, P. Rossi and B. Valtancoli, *J. Chem. Soc., Dalton Trans.*, 2001, 917–922.
31 S. Wang and T. D. Westmoreland, *Inorg. Chem.*, 2009, **48**, 719–728.
32 *Scientist for Windows*, Version 2.0, Micromath Inc., Salt Like City, UT, 1995.
33 (*a*) M. Kývala and I. Lukeš, *International Conference Chemometrics '95*, Pardubice, Czech Republic, 1995, p. 63; (*b*) M. Kývala, P. Lubal and I. Lukeš, *IX. Spanish-Italian and Mediterranean Congress on Thermodynamics of Metal Complexes (SIMEC 98)*, Girona, Spain, 1998.
34 (*a*) A. E. Martell and R. M. Smith, *Critical Stability Constants*, Vols. 1–6, Plenum Press, New York, 1974-1989; (*b*) NIST Standard Reference Database 46 (Critically Selected Stability Constants of Metal Complexes), Version 7.0, 2003; (*c*) C. F. Jr., Baes and R. E. Mesmer, *The Hydrolysis of Cations*, Wiley, New York, 1976.
35 (*a*) P. Táborský, P. Lubal, J. Havel, J. Kotek, J. Rudovský, P. Hermann and I. Lukeš, *Collect. Czech. Chem. Commun.*, 2005, **70**, 1909–1942; (*b*) M. Försterová, I. Svobodová, P. Lubal, P. Táborský, J. Kotek, P. Hermann and I. Lukeš, *Dalton Trans.*, 2007, 535–549.
36 S. Cortes, E. Brücher, C. F. G. C. Geraldes and A. D. Sherry, *Inorg. Chem.*, 1990, **29**, 5–9.
37 H. Hama and S. Takamoto, *Nippon Kugaku Kuishi*, 1975, 1182–1185. CAN: 83:121751, CODEN: NKAKB8, ISSN: 0369-4577.
38 G. Anderegg, F. Arnaud-Neu, R. Delgado, J. Felcman and K. Popov, *Pure Appl. Chem.*, 2005, **77**, 1445–1495.
39 A. Bianchi, L. Calabi, C. Giorgi, P. Losi, P. Mariani, P. Paoli, P. Rossi, B. Valtancoli and M. Virtuani, *J. Chem. Soc., Dalton Trans.*, 2000, 697–705.
40 C. F. G. C. Geraldes, M. C. Alpoim, M. P. M. Marques, A. D. Sherry and M. Singh, *Inorg. Chem.*, 1985, **24**, 3876–3881.
41 G. F. Smith and D. W. Margerum, *Inorg. Chem.*, 1969, **8**, 135–138.
42 S. H. Koenig, C. Baglin, R. D. III. Brown and C. F. Brewer, *Magn. Reson. Med.*, 1984, **1**, 496–501.